Chemistry, Physics and Technology of Surface. 2012. V. 3. N 4. P. 359-374

*UDC 544.723:*577.3:582.282.23

THE BEHAVIOUR OF INTRACELLULAR WATER IN YEAST CELLS AFFECTED BY ORGANIC SOLVENTS

V.M. Gun'ko*, T.V. Krupska, V.M. Barvinchenko, V.V. Turov

Chuiko Institute of Surface Chemistry of National Academy of Sciences of Ukraine
17 General Naumov Str., Kyiv, 03164, Ukraine

Yeast Saccharomyces cerevisiae cells dry (containing approximately 7 wt. % of water) and partially rehydrated (10 wt. % addition of water) and with added organic solvents (10 wt. % or 2–3 g per gram of dry cells) nonpolar (C_6H_6, CCl_4) or polar (CD_3CN, $(CH_3)_2CO$, $(CD_3)_2CO$, $(CH_3)_2SO$, $(CD_3)_2SO$) were studied using ^1H NMR spectroscopy with layer-by-layer freezing-out of bound and bulk liquids at 200–273 K, TG/DTA and FTIR spectroscopy methods. Nonpolar solvents displace a portion of water into narrower 'pores' in contrast to polar solvents which displace water into larger 'mesopores' in the intracellular space. This structural feature of intracellular water is accompanied by its energetic differentiation, and four types of intracellular water are found: weakly (chemical shift δ_H = 1–2 ppm) and strongly associated (δ_H = 3–5 ppm) waters which can be strongly (ΔG < –0.8 kJ/mol) or weakly (ΔG > –0.8 kJ/mol) bound to intracellular functionalities.

INTRODUCTION

Many of microorganisms being under negative environmental conditions can fall into anabiosis accompanied by their strong dehydration and termination of the vital processes during a long period [1–5]. Viable bacteria (eukaryotes: yeasts, fungi, and mosses and different prokaryotes) were found in permafrost soils (up to 10^5–10^7 cells/g) being at $T < 263$ K for a few thousand years up to 2–3 million years [6]. These bacteria populations may be viewed as the result of a continuous process of selection for those capable of withstanding prolonged exposure to subzero temperature, accompanying low water activity, and other special challenges posed by the permafrost as well as the outcome of tens of thousands of years of cyclic freeze-thaw selection in the original "active" tundra layers [7, 8]. When bacteria are exposed to sudden temperature downshifts, two major responses are commonly observed such as changes in membrane lipid composition and production of novel proteins (e.g. Csp family) [9–11]. Key function of cold acclimation is to stabilise membranes against freezing-injury and multiple mechanisms appear to be involved in this stabilisation, e.g. changes in lipid composition, the accumulation of "compatible solutes" (proline and simple sugars), cryoprotective polypeptides (encoded by COR and LEA genes) and antifreeze proteins (with alanine-rich α-helixes, cystine-rich globular, compact β-sheet and four-helix bundle structures) [12–17]. Renewal of the active state after anabiosis occurs on changes in conditions (e.g. appearance of a nutrient medium at appropriate temperature and hydration) corresponding to optimal parameters for the vital activity and cells growth [18]. Rehydration of cells is accomplished sufficiently rapidly [19] that indicate the accessibility of internal space of cells for water molecules and dissolved substances.

Microorganisms being in anabiosis can be subjected to cold stress at temperature of liquid nitrogen at 77.4 K without injury of them. The anabiosis state is reached upon cryopreservation and long storage of cells and tissues at a similar temperature [20–24]. To reduce injury of cells their strong dehydration is implemented upon cryopreservation utilizing low-molecular cryoprotectants similar to that occurring under natural conditions of bacteria anabiosis. This dehydration is caused by the displacement of a significant portion of intracellular water by organic compounds and formation of an intracellular concentrated 'solution' of cryoprotectants in cells. Dehydrated cells can be considered as a complex system with connected nanobiostructures forming pockets ('pores'). In dehydrated cells only a minor portion of these pockets is filled by structured water with dissolved low-molecular organic or inorganic

* corresponding author *vlad_gunko@ukr.net*

compounds. Changes in the environment, e.g. upon hydration of dry cells, lead to appearance of concentration gradients and strong osmotic pressure at the cellular interfaces (membranes and inner structures) that result in fast rehydration of cells. Added organic solvents can easily penetrate into dehydrated or partially rehydrated cells and change the state of intracellular water.

Investigations of yeast S*accharomyces cerevisiae* cells using the ^{1}H NMR spectroscopy with layer-by-layer freezing-out of intracellular liquid phase at $T < 273$ K (partial and temperature-dependent freezing of water is due to colligative properties of water bound in cells and the Gibbs-Thomson relation for the freezing point depression for liquids in confined space) [25, 26] showed that water in partially hydrated cells is in weakly associated state in which the average number of the hydrogen bonds (through the hydrogen atoms) is less than one per a molecule. Similar results were observed for other systems with mosaic hydrophilic/hydrophobic surface functionalities [25–28]. For this water in contrast to bulk one (characterised by the chemical shift of proton resonance (δ_H) close to 5 ppm), the chemical shift is 1.3–2 ppm which corresponds to the δ_H values for water molecules dissolved in nonpolar or weakly polar organic solvents or being in the gaseous state [29–31]. Significant amounts of weakly associated water were also found in bone tissues [32, 33] and at the interfaces of hydrated partially functionalised oxide nanoparticles placed in weakly polar organic solvents [27, 34]. The properties of this water strongly differ from that of bulk water, e.g. it freezes at $T < 220$ K and can form specific mixtures with weakly polar solvents in pores, especially at mosaic hydrophobic wall surfaces [27].

The aim of this paper was to study the effects of nonpolar (C_6H_6, CCl_4) and polar (CD_3CN, $(CH_3)_2CO$, $(CD_3)_2CO$, $(CH_3)_2SO$, $(CD_3)_2SO$) organic solvents on the structure and the Gibbs free energy of intracellular water in yeast S*accharomyces cerevisiae* cells using the ^{1}H NMR spectroscopy with layer-by-layer freezing-out of bulk and intracellular liquids, FTIR spectroscopy and TG/DTA methods for deeper understanding the mechanism and features of the processes occurring on cell cryopreservation.

EXPERIMENTAL

Materials. Commercial dry yeast *Saccharomyces cerevisiae* cells were chosen because of their viability on drying/rehydration and freezing/thawing. For the investigations, dry yeast cells (containing approximately 7 wt. % of water) were used as the initial material and then wetted by a given amount of water and organic solvents. In the majority of the experiments, the same amount of water (10 wt. %) was added to cell granules (diameter ~0.25 mm) then equilibrated for seven days in closed dishes at room temperature.

Proton-containing and deuterated organic solvents (Aldrich) were added to partially hydrated cells (mass 300–400 mg) directly into the NMR ampoules shaken for 10 min and equilibrated for 1 h. Then ampoules were placed into the NMR spectrometer and temperature was decreased to 200–210 K for 15 min and then it was elevated by a step of 5–10 K and samples were equilibrated at each temperature for 5 min under thermostatic control. Each temperature at $T < 273$ K corresponds to certain balance between frozen and unfrozen water fractions in cells depending on features of its interaction with intracellular functionalities.

^{1}H NMR spectroscopy and NMR-cryoporometry. The ^{1}H NMR spectra of intracellular water were recorded at 210–280 K using a Varian 400 Mercury spectrometer of high resolution with the probing 90^o pulses at duration of 2 μs. The temperature was controlled (±1 K) by means of a Bruker VT-1000 device. Relative mean errors were ±10 % for ^{1}H NMR signal intensity. To prevent supercooling of cells, the measurements of the amounts of unfrozen water ($C_{uw}(T)$) were carried out on heating of samples preliminarily cooled to 210 K. The ^{1}H NMR spectra recorded here include the signals only of unfrozen mobile water and low-molecular organic molecules (in the H form). The signals of water molecules from ice, as well as protons from cellular macromolecules and other structures, do not contribute the ^{1}H NMR spectra because of features of the measurement technique (bandwidth ≤ 10 kHz) and the short duration (~10^{-6} s) of transverse relaxation of protons in immobile structures which is shorter by several orders than that of mobile water or organic molecules [26, 35].

Changes in the Gibbs free energy of ice [36] depend on temperature as follows

$$\Delta G_{ice}(T)\ (\text{kJ/mol}) = 0.0295 – 0.0413\Delta T + \\ + 6.64369\times10^{-5}(\Delta T)^2 + 2.27708\times10^{-8}(\Delta T)^3, \quad (1)$$

where $\Delta T = 273.16 - T$ at $T \le 273.15$ K (correlation coefficient is equal to 0.9999). The $\Delta G(T)$ and $C_{uw}(T)$ functions can be easily transformed into the relationship $\Delta G(C_{uw})$ [26]. The area under the $\Delta G(C_{uw})$ curve determines overall changes in the Gibbs free energy of interfacial water (interfacial free energy)

$$\gamma_S = A \int_0^{C_{uw}^{max}} \Delta G dC_{uw}, \qquad (2)$$

where C_{uw}^{max} is the total amount of unfrozen water at $T = 273.15$ K and A is a constant dependent on the type of units used in Eq. (2). Weakly bound water (WBW) corresponding to a portion of unfrozen water with the Gibbs free energy slightly lowered by intermolecular interactions with cell structures freezes at a temperature close to 273 K. Strongly bound water (SBW) can be unfrozen even upon significant cooling of the system and corresponds to the maximum disturbed water layer at the interfaces. The thickness of the layers of each type of water (C^s_{uw} and C^w_{uw} for SBW and WBW, respectively) and the maximum values for lowering of the free energy of these waters (ΔG_s and ΔG_w) can be estimated from a linear extrapolation of appropriate linear portions of the $\Delta G(C_{uw})$ graphs to the corresponding axis [26, 35]. Notice that there are two types of water amounts: unfrozen fraction (C_{uw}) and total amount (C_{H2O}). The amounts of weakly (WAW, C_{uw}^{wa}) and strongly (SAW, C_{uw}^{sa}) associated bound waters as a function of temperature were calculated by integrating the corresponding peaks at $\delta_H = 1.3$–2 ppm and 3.5–5 ppm, respectively, from decomposed (using the Gaussian functions) total ^{1}H NMR spectra recorded at different temperatures.

Water or other liquids can be frozen in narrower pores (i.e. more strongly bound and structured) at lower temperatures that can be described by the Gibbs-Thomson (GT) relation for the freezing point depression [37–40]

$$\Delta T_m = T_m(R) - T_{m,\infty} = \frac{2\sigma_{sl} T_{m,\infty}}{\Delta H_f \rho R} = -\frac{k}{R}, \qquad (3)$$

where $T_m(R)$ is the melting temperature of a frozen liquid in pores of radius R, $T_{m,\infty}$ the bulk melting temperature, ρ the density of the solid, σ_{sl} the energy of solid-liquid interaction, ΔH_f the bulk enthalpy of fusion, and k is a constant. In the case of the size of the liquid structures larger than 2–3 nm, the GT relation causes gradual freezing of them; i.e., freezing-out of liquids in confined space occurs layer-by-layer (step-by-step). Equation (3) can be transformed into differential equation assuming that $\frac{dV_{uw}(R)}{dR} = \frac{dC_{uw}}{dR}$ and using $\frac{dT_m(R)}{dR} = \frac{k}{R^2} = \frac{(T_m(R) - T_{m,\infty})^2}{k}$ giving

$$\frac{dV_{uw}(R)}{dR} = \frac{A}{k}(T_m(R) - T_{m,\infty})^2 \frac{dC_{uw}(T)}{dT}, \qquad (4)$$

where $V_{uw}(R)$ is the volume of unfrozen water in pores of radius R, C_{uw} is the amount of unfrozen water per gram of adsorbent as a function of temperature and A is a constant [41–43]. Eqs. (3) and (4) can be transformed into an integral equation on replacing $dV_{uw}(R)/dR$ by $f_V(R)$, converting dC_{uw}/dT to dC_{uw}/dR using $dT = \frac{dT}{dR} dR$ and integrating by R (IGT equation)

$$C_{uw}(T_m) = A' \int_{R_{min}}^{R_{max}} \left(\frac{k}{(T_{m,\infty} - T_m(R))R} \right)^2 f_V(R) dR, \qquad (5)$$

where R_{max} and R_{min} are the maximal and minimal pore radii (or sizes of unfrozen liquid structures) on integrating (here 50 and 0.25 nm), respectively, and A' is a normalisation factor dependent on the values of units used in Eq. (5) [41–43]. Eq. (5) can be solved using a regularisation procedure based on the CONTIN algorithm [44] under nonnegativity condition ($f(R) \ge 0$ at any R) and a fixed or unfixed value of the regularisation parameter (α) determined on the basis of the F-test and confidence regions using the parsimony principle. Notice that this approach based on the GT and IGT equations was applied to many different materials (porous and nonporous silicas, carbon adsorbents, biomacromolecules, soft biomaterials, cells, tissues, seeds, etc.) [25–28, 32, 33, 37–43, 45–48]; and comparison with the results of standard methods (adsorption, microscopic imaging, etc.) for solid adsorbents showed good agreement between them. Therefore, the application of this approach to some objects such as yeast cells which cannot be studied using standard adsorption methods is justified.

The pore size distribution function $f_V(R)$ can be converted into the distribution function $f_S(R)$ with respect to the specific surface area

$$f_S(R) = \frac{w}{R}\left(f_V(R) - \frac{V(R)}{R}\right), \quad (6)$$

where w is a constant dependent on the pore shape. Integration of the $f_S(R)$ function over the total pore size range gives the specific surface area (S_w, Table 1) of the cellular structures being in contact with bound water.

Table 1. Characteristics of cell structures in contact with bound intracellular water unfrozen at $T < 273$ K in cells in different media

Medium	S_w, m^2/g	$S_{w,mic}$, m^2/g	$S_{w,mes}$, m^2/g	$S_{w,mac}$, m^2/g	$V_{w,mic}$, cm^3/g	$V_{w,mes}$, cm^3/g	$V_{w,mac}$, cm^3/g	γ_s, J/g
Air	137	114	22	1	0.035	0.107	0.28	8.3
C_6H_6	462	428	33	0	0.100	0.070	0	10.0
CCl_4	162	98	63	1	0.034	0.117	0.019	5.9
$(CD_3)_2CO$[a]	48	6	37	5	0.001	0.047	0.122	19.0
CD_3CN[a]	88	11	77	0	0.004	0.160	0.005	5.1
$(CD_3)_2SO$[a]	79	3	76	0	0.001	0.168	0.001	7.0

Note. C_{H2O} = 17 wt % in all samples, [a]10 wt % of organic solvents and air medium

Integration of the $f_V(R)$ and $f_S(R)$ functions at $R < 1$ nm, $1 < R < 25$ nm, and $R > 25$ nm gives the volume and the specific surface area of micro-, meso-, and macropores, respectively. The S_w values can be determined from the amount of intracellular water C_{uw}^{max} (estimating pore volume as $V_w = C_{uw}^{max}/\rho_{uw}$) at $T \to 273.15$ K and pore size distribution $f(R)$ (used to estimate the average pore radius R_{av}) with a model of cylindrical pores (used for simplicity)

$$S_w = 2V_{uw}/R_{av} = 2C_{uw}^{max}\int_{R_{min}}^{R_{max}} f(R)dR/(\rho_{uw}\int_{R_{min}}^{R_{max}} f(R)RdR). \quad (7)$$

It should be noted that there is certain limitation of application of Eq. (7) for broad pores ($R > 10$ nm) in which water located far from the pore walls can freeze at $T \approx 273.15$ K because it cannot sense the influence of the distant walls. Therefore, in this case the S_w value can be understated but less than the V_w value because narrower pores are responsible for the maximal contribution to the S_w value but broader pores more strongly contribute the V_w value [41–43].

Thermogravimetry (TG). Thermal analysis of yeast cells initial and after addition of water (10 wt %) and benzene (10 or 170 wt. %) (sample weight ≈ 0.2 g) was carried out in air at 293–1273 K using a Q-1500D (Paulik, Paulik & Erdey, MOM, Budapest) apparatus with TG-DTA (differential thermal analysis) at a heating rate of 10 K/min.

Fourier Transmission Infrared Spectroscopy (FTIR). The FTIR spectra (diffuse reflectance mode) of initial cells (sample 1) and after addition of 10 wt. % of water (sample 2), 10 (3) or 170 (4) wt. % of benzene to sample 2 (mixed with KBr as 1 : 5) were recorded at room temperature using a FTIR ThermoNicolet spectrophotometer.

RESULTS AND DISCUSSION

According to TG/DTA (Fig. 1) and FTIR (Figs. 2 and 3) data, addition of water (10 wt. %) and benzene (10 or 170 wt. %) leads to changes in the behaviour and organisation of intracellular water. Added water enhances the endothermic effect of the water desorption (Fig. 1, *c*, a DTA minimum at 144 °C). However, a DTG minimum (related to a maximal rate of water desorption) shifts towards lower temperatures (by ~5 °C). This difference in the DTG and DTA changes reveals complex organisation of intracellular water dependent on its amounts. Addition of water does not affect a maximum of oxidation of cells at 305 °C. Benzene (used here as a representative nonpolar organic solvent) desorbs from cells easily than water that is well seen at its maximal concentration (Fig. 1, sample 4). Benzene slightly shifts the oxidation maximum (by 2–3 °C) towards lower temperatures because of the loosening effects on intracellular structures.

Deconvolution of the FTIR spectra was done over the range of the O–H stretching vibrations at 2200–3800 cm^{-1} (Fig. 2) to five bands at 3600–3630 cm^{-1} (peak 1, P1), 3500–3550 (P2), 3280–3370 (P3), 2850–2950 (P4), and 2500–2540 cm^{-1} (P5) (in this range, the C–H bands were decomposed too but not analysed here).

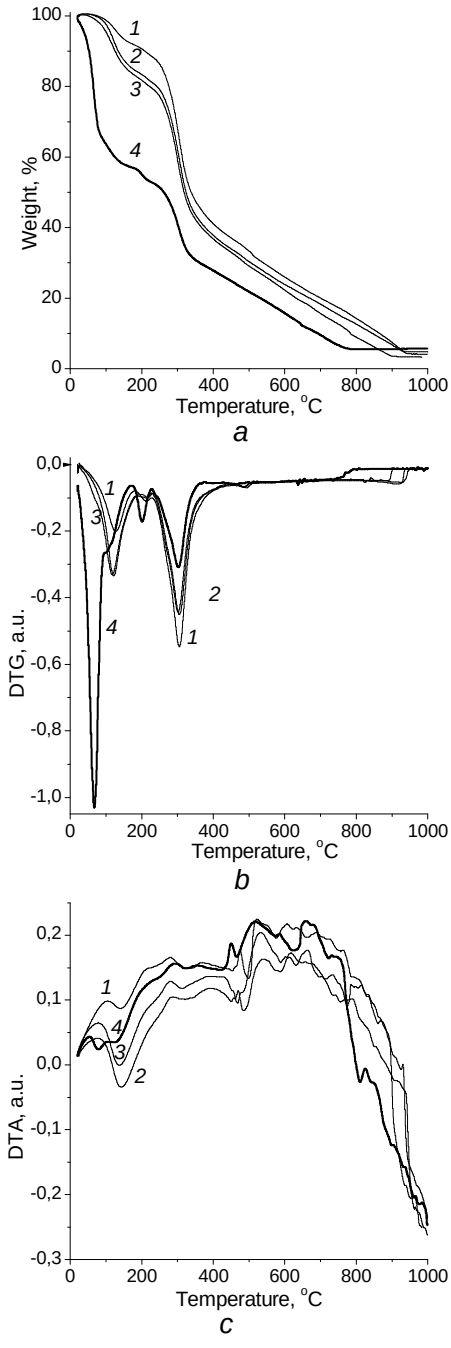

Fig. 1. TG *(a)*, DTG *(b)*, and DTA *(c)* curves for initial yeast cells (curves *1*), after addition of 10 wt. % of distilled water *(2)*, and subsequent addition of benzene of 10 wt. % *(3)* or 170 wt. % *(4)*

These bands can be assigned to more strongly disturbed OH groups (i.e. more strongly bound and strongly associated waters) with decreasing ν_{OH} values. In other words, the band at 2500 cm^{-1} is connected to the most SAW and SBW (e.g. water interacting with charged functionalities, structures with attached protons, disturbed acidic COOH groups, etc.), but the band at 3600 cm^{-1} is linked to WAW. Several effects are observed on addition of water (sample 2) and benzene (samples 3 and 4) (Figs. 2 and 3). Addition of water diminishes the amounts of WAW because contribution of peaks 1–3 decreases and the amounts of SBW and SAW increase (peaks 4 and 5). Addition of the low amount of benzene differently affects intracellular water and contribution of the most SBW grows (Fig. 3, curve 5, sample 3). The increase in benzene content leads to a small decrease in contribution of SBW (curves 5 and 4) and WAW (curves 2 and 3). More detailed analysis of re-organisation of intracellular water could be done on the basis of the ^{1}H NMR investigations of yeast cells on addition of water and different organic solvents.

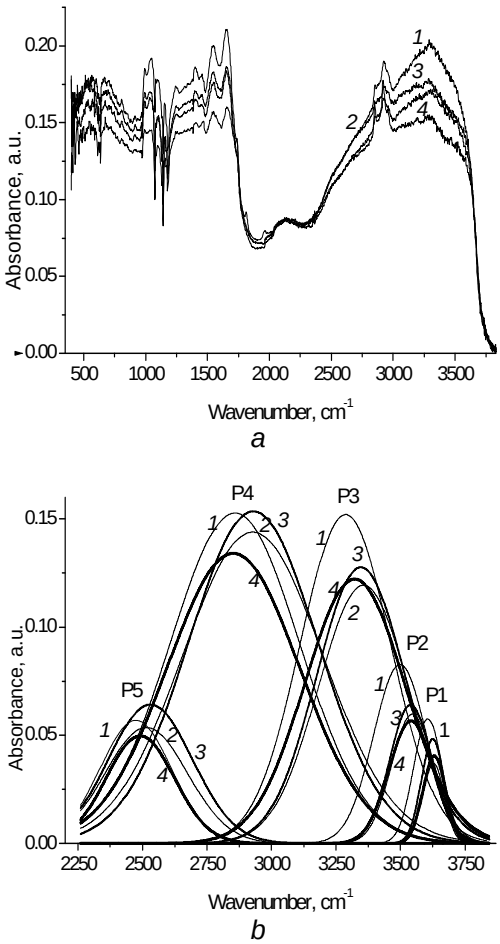

Fig. 2. FTIR spectra *(a)* of initial yeast cells (curves *1*), after addition of 10 wt. % of distilled water (*2*), and subsequent addition of benzene of 10 wt. % (*3*) or 170 wt. % (*4*); deconvolution of the spectra to five bands over the O–H stretching vibrations *(b)*

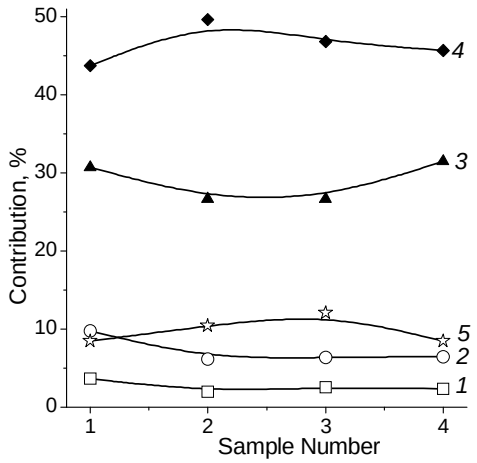

Fig. 3. Contribution of five OH bands (shown in Fig. 2, *b*) into the spectra at 2200–3860 cm^{-1}

Fig. 4 shows the ^{1}H NMR spectra of water bound in initial dry yeast cells (at low hydration C_{H2O} = 7 wt. %) recorded at different temperatures.

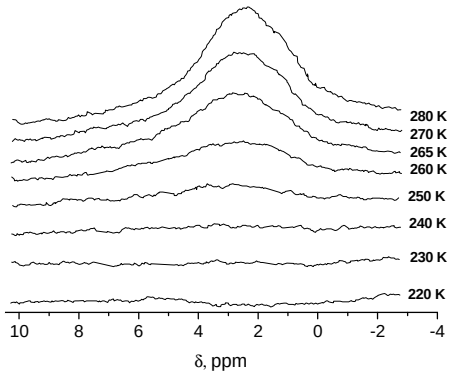

Fig. 4. ^{1}H NMR spectra of water (7 wt. %) in yeast cells at different temperatures

The spectra include a single signal with the chemical shift at $\delta_H \approx 1.5$–3 ppm, i.e., a major portion of this water could be assigned to WAW which freezes at $T > 250$ K. In accordance with Eq. (1), a decrease in the Gibbs free energy of this fraction of structured water is smaller than 1 kJ/mol (i.e. $\Delta G > -1$ kJ/mol); consequently, it can be also attributed to WBW. A similar shape and temperature behaviour of the ^{1}H NMR spectra (not shown here) is observed for cells containing 17 wt. % of water. Notice that this water content is insufficient to provide renewal of the vital processes in cells; i.e. their state at the used temperatures can be considered as a state appropriate for cryopreservation. To analyse the effects caused by low-molecular organics (some of them, e.g. DMSO, can be used as cryoprotectants) penetrating into cells, partially hydrated yeast cells were studied after addition of a relatively low amounts of benzene, acetone, DMSO, acetonitrile, carbon tetrachloride, and methane, or cells being in the organic medium (2–3 g per gram of cells).

Yeast cells are capable to absorb significant amounts of organic solvents and gaseous methane. Fig. 5, *a* shows the ^{1}H NMR spectra of yeast cells containing 17 wt. % of water after being in a methane flow (rate 50 ml/min) for 30 min. The ^{1}H NMR signal of methane (0.5 wt. % with respect to cell weight) at $\delta_H \approx 0$ ppm is well observed in the spectra at $T < 250$ K when the signal of water becomes very low; however, at $T \geq 250$ K both signals overlap. Thus, adsorbed methane does not affect intracellular water which remains weakly associated and weakly bound similar to that in the initial cells (Fig. 4).

Figs. 5, *b*, *c* show the ^{1}H NMR spectra of water in yeast cells placed in CCl_4 and benzene (signal of benzene is observed at $\delta_H \approx 7.2$ ppm) media, respectively. These solvents can penetrate into cells that lead to significant changes in the ^{1}H NMR spectra of adsorbed water, i.e. its organisation changes. A fraction of intracellular water affected by the solvents becomes strongly associated and characterised by the signal at $\delta_H \approx 5$ ppm. Another portion of water remains weakly associated and characterised by the signal at $\delta_H \approx 1.2$ ppm. In the case of added benzene, the signal of SAW is observed as a shoulder on the right wing of the benzene signal. Additionally, intracellular water becomes strongly bound because it freezes at much lower temperatures than that in the initial cells. The observed effects can be considered as the result of structural differentiation of intracellular water.

Fig. 6 depicts the temperature dependences of concentration of WAW (Fig. 6, *a*) and the dependences of changes in the differential Gibbs free energy of WAW (Fig. 6, *b*) and SAW (Fig. 6, *c*). The replacement of air by a nonpolar organic solvent leads to a considerable decrease in the amounts of WAW (Fig. 6, *a*) (by two times for benzene and five times for CCl_4). This occurs due to the transformation of a fraction of WAW into SAW. Additionally, there is the transformation of a fraction of WAW from WBW to SBW which does not freeze even at 210 K (especially in the case of benzene, Fig. 5, *c*). However, a portion of SAW remains weakly bound ($\Delta G > -1$ kJ/mol).

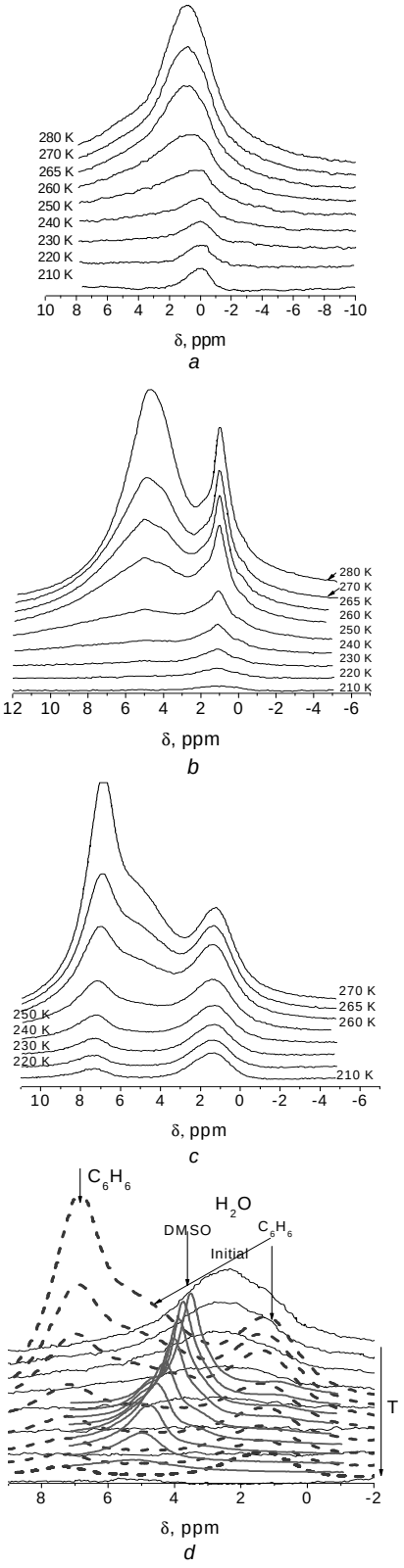

Fig. 5. ^{1}H NMR spectra of intracellular water (17 wt. %) and methane *(a)*, and for yeast cells (17 wt. % of water) being in CCl_4 *(b)*; C_6H_6 *(c)* media at different temperatures; comparison of the spectra of initial cells and cells in C_6H_6 and DMSO-d_6 media *(d)*

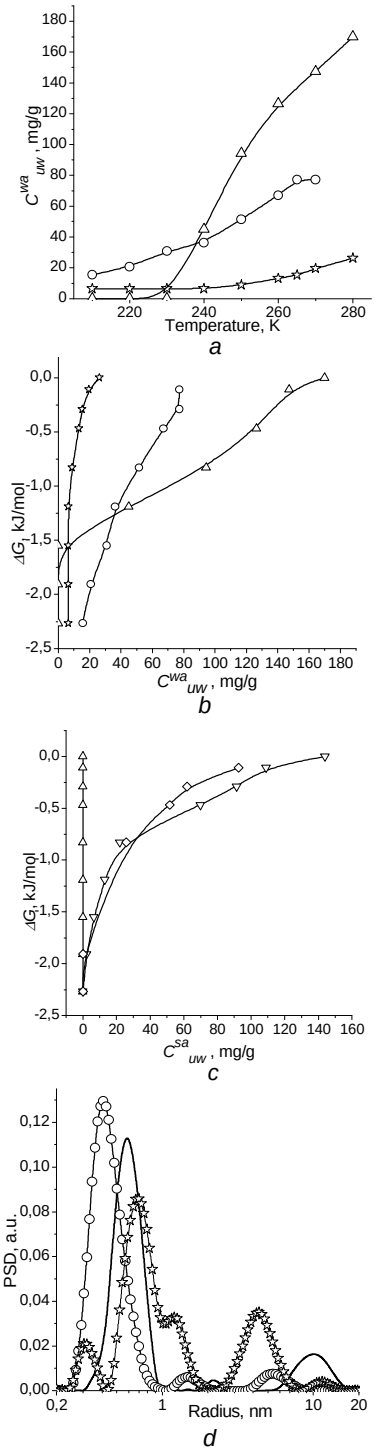

Fig. 6. The temperature dependences of concentration of weakly associated water C_{uw}^{wa} *(a)* and changes in the Gibbs free energy of weakly associated water *(b)*, strongly associated water C_{uw}^{sa} *(c)* in yeast cells containing 17 wt. % of water in air – △ , CCl_4 – ☆ and benzene – ○ , and pore size distribution functions *(d)* calculated using Eq. (5)

Thus, energetic differentiation of intracellular water affected by nonpolar organic solvents occurs together with its structural differentiation (Figs. 5 and 6). This phenomenon is analogous to that observed previously on self-organisation of the water/organic mixtures in confined space of pores with mosaic hydrophilic/hydrophobic walls in microporous activated carbons [45, 46], ordered mesoporous silicas [47] and fumed silicas [48]. These re-arrangements of bound water occur under the principle of minimisation of the Gibbs free energy of the systems on interactions of hydrophilic/hydrophobic functionalities with water and organic solvents as well as between molecules in the mobile liquid phases. In the case of water/nonpolar solvent condition of a minimal surface area of their contact is predominant. To reach this the organic solvent can displace water into larger pores (to form WBW-SAW structures such as nanodroplets or microdomains) or into very narrow pores (pockets) with hydrophilic/hydrophobic walls (to form SBW-WAW which interacts with hydrophilic patches of the walls but nonpolar organic solvent molecules interact mainly with nonpolar hydrophobic patches). Fig. 5, *b* shows that the signals of WAW-SBW and strongly bound benzene are observed in the cells at very low temperatures. The PSD functions (Fig. 6, *d*) and the structural characteristics (Table 1) reveal that the effects of benzene and CCl_4 on intracellular water strongly differ. For instance, benzene and CCl_4 causes the displacement of the micropore peak towards opposite directions and the PSD functions for mesopores differ too because CCl_4 enhances location of water in mesopores but benzene promotes water location in micropores (Fig. 6, *d*, Table 1).

Fig. 7 shows the ^{1}H NMR spectra of water and methyl groups in acetone and DMSO (for the proton-containing solvents) and only water in the case of the deuterated form of polar solvents added to cells. In contrast to nonpolar solvents (CCl_4 and C_6H_6), these organic compounds possess high electron-donor ability and, therefore, can form mixtures with water at any concentration in the bulk. Water dissolved in these organics at excess of them is characterised by the average chemical shifts at $\delta_H \approx 2.5$–3.0 ppm. Intracellular water in yeast cells being in the acetonitrile medium (Fig. 7, *a*) gives two signals at $\delta_H \approx 1$ and 3 ppm.

These water structures can be assigned to WAW in contact with intracellular functionalities and water dissolved in acetonitrile (in cells or out of cells). The intensity of the latter changes weakly with lowering temperature from 280 to 240 K and it vanishes at $T \le 230$ K because of freezing-out of an eutectic mixture with water-acetonitrile ($T_{m,\infty}(CD_3CN) \approx 230$ K). The signals of WAW and water dissolved in acetonitrile are observed separately, i.e., the molecular exchange between these waters occurs slowly in the NMR time scale [29]. Consequently, these water structures can be spatially separated. Since the content of acetonitrile (approximately 2 g per gram of cells) in the sample was higher by order than that of water, the signal of water dissolved in acetonitrile has a large width and strongly diminishes at $T \le 230$ K, one can conclude that a minor portion of water dissolved in acetonitrile remains in the intracellular space. As in the case of nonpolar solvents a fraction of WAW transforms from WBW into SBW which does not freeze at $T > 210$ K. SAW is absent in yeast cells immersed in liquid acetonitrile. Notice that the structures with SAW (i.e. relatively large structures) are rather undesirable on cryopreservation of cells because of the negative effects of ice crystallites resulting in injury of cells.

Addition of 10 wt. % of acetone and DMSO (possessing stronger electron-donor properties than acetonitrile but much higher $T_{m,\infty}(\text{DMSO}) \approx 291$ K or much lower $T_{m,\infty}(\text{acetone}) \approx 179$ K) to the cells (Fig. 7) leads to appearance of the signals of SAW and WAW (signal of methyl groups is also observed in the case of the solvents in the H-form). The ^{1}H NMR spectra of water on addition of deuterated acetone and DMSO are close at high temperatures (Fig. 7) but a larger difference is observed at $T < 260$ K. At low temperatures, WAW is stabilised in the cells containing acetone (Fig. 7, *c*) but mainly SAW is observed in the cells with DMSO (Fig. 7, *e*).

Water dissolved in DMSO is observed only in the case of great excess of the solvent (Fig. 7, *f*). At $T = 280$ K (lower than the freezing point of bulk DMSO at 291.5 K) there are three signals of water at $\delta_H \approx 1$, 3 and 5 ppm corresponding to WAW, water dissolved in DMSO and SAW, respectively. Water dissolved in DMSO transforms into SAW with lowering temperature, probably, because of the DMSO crystallisation and pressing-out of dissolved water on the outer surface of DMSO crystallites.

The chemical shift of this water increases from 3 to 5 ppm and the second and third signals are observed as a single signal that indicate the existence of fast molecular exchange between both forms of water. Weak signals of SAW (a shoulder at $\delta_H \geq 5$ ppm) and WAW ($\delta_H \approx 1$ ppm) are observed at $260 < T < 280$ K (Fig. 7, *f*) and their intensity changes weakly in this temperature range. This behaviour of the ^{1}H NMR spectra can be explained by the fact that these waters locate in pores (pockets) of different sizes with the walls of different chemical structures with hydrophilic and hydrophobic functionalities.

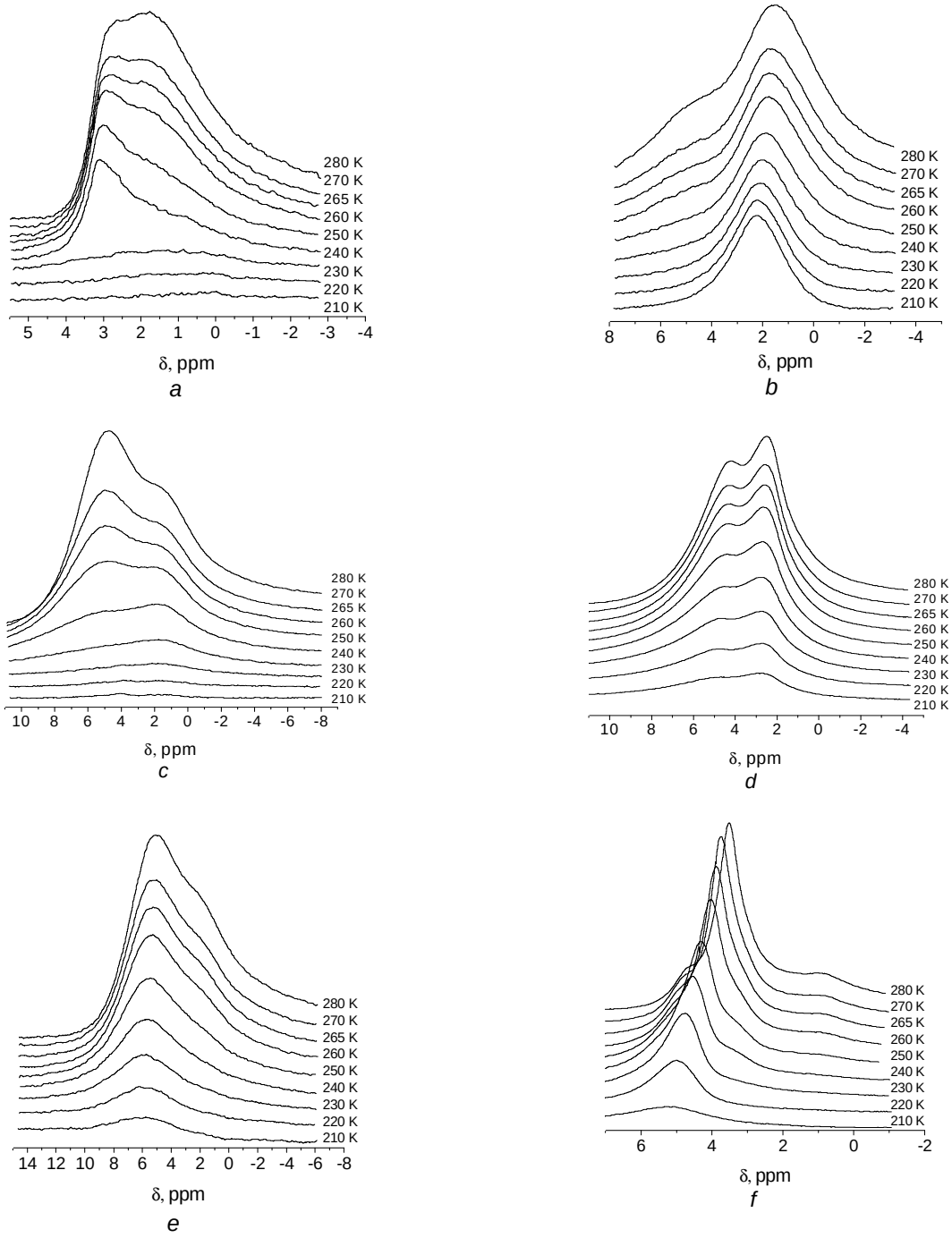

Fig. 7. ^{1}H NMR spectra of water (17 wt. %) in yeast cells in CD_3CN medium*(a)*, and on addition of 10 wt. % of $(CH_3)_2CO$ *(b)*, $(CD_3)_2CO$*(c)*, $(CH_3)_2SO$ *(d)*, $(CD_3)_2SO$ *(e)* and in $(CD_3)_2SO$ *(f)* medium at different temperatures

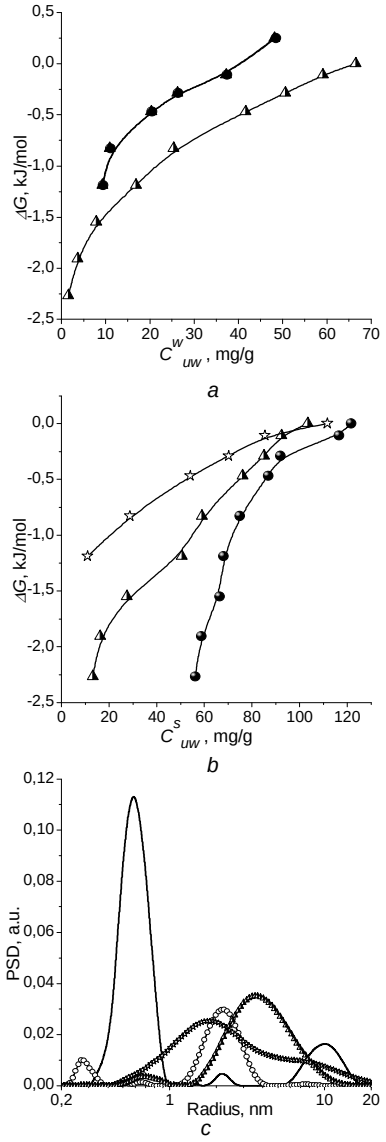

Fig. 8. Changes in the Gibbs free energy as a function of the content of unfrozen water for weakly associated *(a)* and strongly associated *(b)* water in yeast cells containing 17 wt. % of water and 10 wt. % of $(CD_3)_2SO$ – △ , $(CD_3)_2CO$ – ● and CD_3CN – ☆ ; and corresponding PSD functions *(c)*

These pores are spatially separated; therefore, the molecular exchange of water between them does not occur. Comparison of the spectra of initial cells and cells in the benzene and DMSO media (Fig. 5, *d*) reveals a significant difference in the effects of nonpolar (C_6H_6) and polar (DMSO) solvents on the organisation of intracellular water. The associativity of water in cells in the DMSO medium is much higher than that in the benzene medium; in other words, clusterisation of intracellular water is stronger in cells being in the benzene medium.

Fig. 8 shows the dependences $\Delta G(C_{uw})$ for WAW and SAW in yeast cells containing 17 wt. % of water and 10 wt. % of organics, the total content of unfrozen water as a function of temperature $C_{uw}(T)$ and the corresponding PSD functions calculated using Eq. (5). The influence of acetonitrile and acetone results in the transformation of WAW into WBW; however, with the presence of DMSO-d_6, WBW gives approximately 60 % of WAW. The dependences $\Delta G(C^w_{uw})$ for acetone and acetonitrile coincides but in the case of DMSO-d_6 the corresponding dependence shifts towards lower Gibbs free energy by approximately –0.7 kJ/mol. Approximately half of SAW corresponds to SBW with the presence of acetone and DMSO-d_6 in the cells, and in the case of acetonitrile, 90 % of SAW is WBW. All polar solvents displace bound water into larger mesopores (Fig. 8, *c* and Table 1) in contrast to nonpolar solvents (Fig. 6, *d*). This difference can be caused by the possibility of the formation of mixtures of these solvents with water at any concentration in the bulk. However, the capability of interfacial water to dissolve organics diminishes [49–51]; therefore, the formation of the separated structures with water and organic solvents is possible in the intracellular space even in the case of polar solvents.

In the case of the cellular suspensions, the shape of the temperature dependences of the ^{1}H NMR signal intensity of unfrozen water (Fig. 9, *a*) is similar to that observed for aqueous suspensions of macromolecules and nanooxides [26, 50, 51]. A maximal intensity of bound unfrozen water is observed at a minimal amount of water (73 wt. %, practically all water is intracellular) because in this case a relative content of bulk water (~40 %) is minimal. Notice that the C_{uw} values are attributed to both intracellular and extracellular waters. Therefore, the γ_S values (Table 2) could be calculated per gram of dry cells. On the basis of the data shown in Table 2, one can conclude that there is no a simple correlation between the amount of water and the characteristics of bound water. An increase in the cell content in the suspension leads to a decrease in the amounts of bound water and the γ_S value; however, these changes are nonlinear.

Table 2. Characteristics of unfrozen water bound in yeast *S. cerevisiae* cells being in the aqueous suspensions of different concentration

	C_{cell}+C_{ICW}, wt. %							
Parameter	3.0	4.5	6.1	10.0	12.5	25.0	50.0	100.0
C_{H2O}, wt. %	99.2	98.8	98.4	97.3	96.6	93.2	86.5	73.0
$-\Delta G_s$, kJ/mol	3.19	3.99	3.34	3.80	3.89	2.73	3.19	3.35
$-\Delta G_w$, kJ/mol	0.9	0.8	0.9	0.7	0.8	0.8	0.8	0.7
C_{uw}^{s}, mg/g	1500	950	820	600	750	900	750	700
C_{uw}^{w}, mg/g	2888	2983	1878	3105	2152	1997	1671	1923
$C_{uw,max}$ mg/g	4388	3933	2698	2705	2902	2897	2421	2623
γ_S, J/g	208.3	168.9	123.3	137.7	139.9	119.2	106.8	97.4
$<T>$, K	247.9	245.3	248.8	245.6	246.6	252.0	249.9	252.8
S_{uw}, m^2/g	1551	1641	840	1181	1182	593	769	643
S_{nano}, m^2/g	1217	1279	623	916	941	379	577	439
S_{meso}, m^2/g	323	362	208	265	241	209	185	193
S_{macro}, m^2/g	11	0	8	0	0	5	6	12
V_{nano}, cm^3/g	0.519	0.488	0.260	0.360	0.366	0.175	0.246	0.182
V_{meso}, cm^3/g	3.490	2.492	2.190	2.050	2.212	2.543	1.984	2.105
V_{macro}, cm^3/g	0.151	0	0.106	0	0	0.081	0.082	0.147

Note. C_{H2O} is the total content of intra- and extracellular water, C_{ICW} is the content of intracellular water (ICW), C_{cell} is the weight of dry cells, nanopores at radius $R < 1$ nm, mesopores at $1 < R < 25$ nm, macropores at $R > 25$ nm, average freezing temperature $<T> = \int I(T)T\mathrm{d}T/\int I(T)\mathrm{d}T$, $I(T)$ is the temperature dependence of the integral intensity of ^{1}H NMR signal of water unfrozen at T

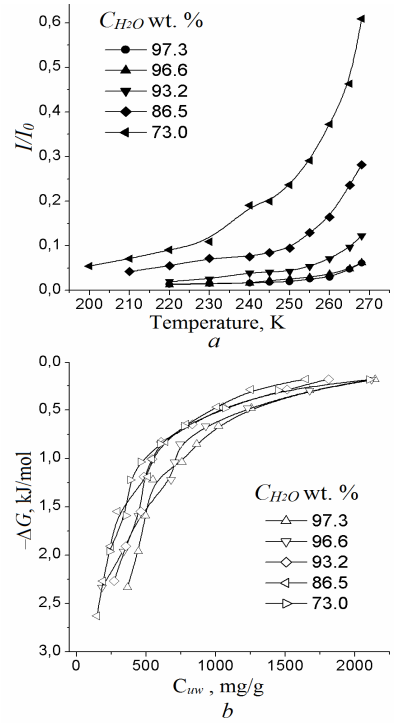

Fig. 9. Temperature dependences of relative intensity (normalized to the water signal, I_0 at 275 K before sample freezing) of the ^{1}H NMR signal of unfrozen water for frozen aqueous suspensions of yeast cells at different total content of water *(a)*; and the corresponding relationships between the amounts of unfrozen water C_{uw} and changes in the Gibbs free energy of bound water *(b)*

The most extremum behavior of all the characteristics is observed at low content of cells in the suspension (Fig. 10).

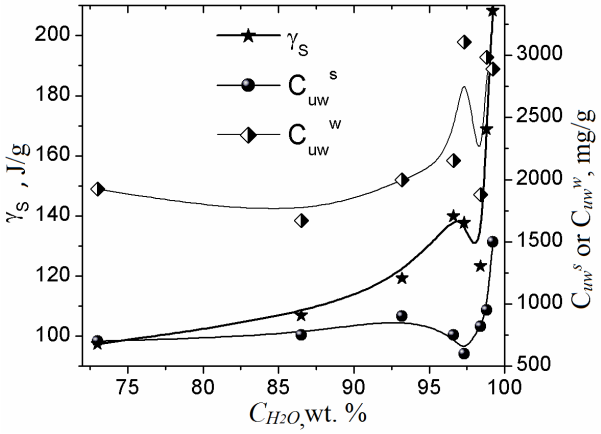

Fig. 10. Relationships between total content of water and changes in the free surface energy and the amounts of strongly and weakly bound waters in yeast cells suspensions

A minimum of γ_S and C_{uw}^{s} and a maximum of C_{uw}^{w} are at $C_{H2O} = 98.4$ wt. % or $C_Y = C_{cell} + C_{ICW} = 6.1$ wt. %. Notice that there is the extreme dependence of the γ_S value on the total concentration of water in the aqueous suspensions of nanooxides [50, 51] at a minimum at $C_{H2O} \approx 93$ wt. %. This boundary concentration corresponds to transition from diluted suspensions to concentrated ones characterized by different particle-particle interactions. In the

diluted suspensions, the systems can separate into a gel-like layer and upper layer with bulk, almost pure water. In the concentrated suspensions, the systems represent a continuous gel-like structure without separation of bulk water. With increasing size of particles the critical concentration (C_c) should increase. Therefore, one could expect a larger C_c value for yeast *S. cerevisiae* cells (5–10 μm) than for nanosilica (primary particles ~ 10 nm). However, the C_c values for yeast cells and nanosilica are relatively close due to the formation of silica nanoparticles aggregates ~ 0.5–1 μm and agglomerates > 1 μm which have sizes close to sizes of cells.

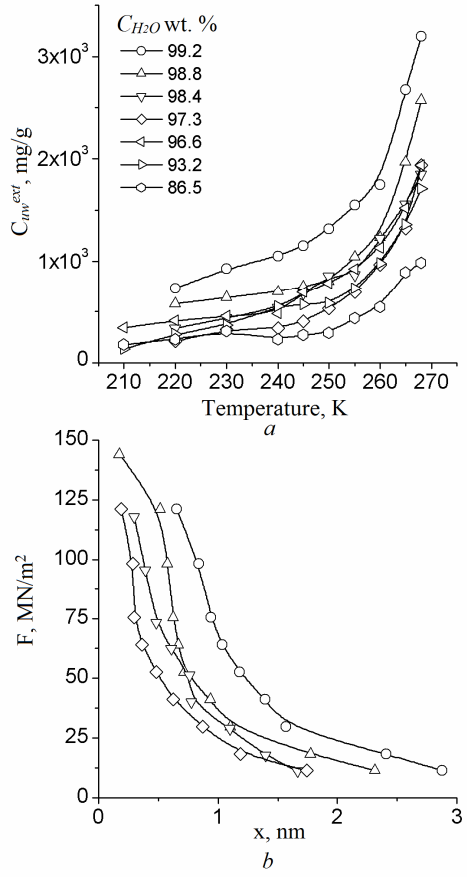

Fig. 11. Changes in the content of unfrozen extracellular water *vs.* temperature *(a)* and radial forces of adhesion of water layers for more diluted systems *(b)*

Therefore, at $C_Y < 10$ wt. % ($C_Y < C_c$) the systems represent colloidal dispersion with relatively weak inter-cell interactions. At these C_Y values the adhesion forces for bound water can be calculated. The distance from the cell surface (x) can be calculated in approximation of a plane interface

$$x \text{ (nm)} = 0.9\, C_{uw}^{ext}/S, \qquad (8)$$

where S is the external specific surface area of cells (estimated as 1 m^2/g for a smooth cell surface) and C_{uw}^{ext} is the amount of extracellular water (Fig. 11). In this approach, the adhesion forces for the cell suspensions are much stronger than that for nanooxides [35, 45, 50]. This difference can be explained by the use of too small S value in Eq. (8). Real specific surface area of the cells is much larger because of a significant nanoscaled roughness of the cell surface than that estimated for the smooth cell surface. The estimation of the S value using NMR cryoporometry as the surface area in contact with unfrozen water (Table 2, S_{uw}) gives very large values which, however, significantly change with changing hydration degree of cells.

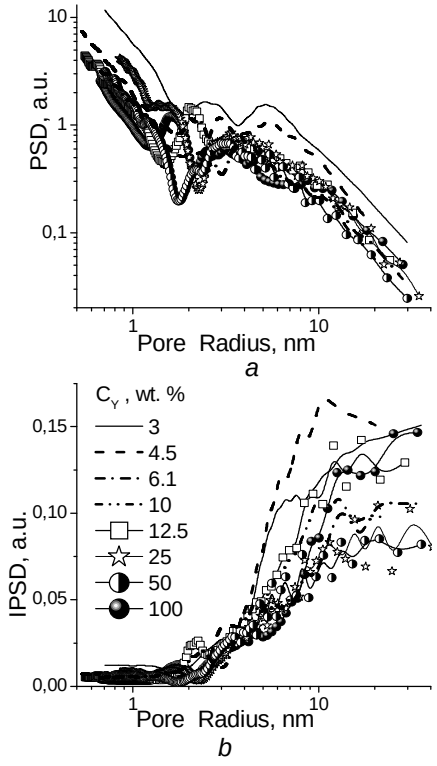

Fig. 12. Size distributions *a* differential and *b* incremental of pores filled by unfrozen water (cylindrical pore model) bound in strongly hydrated yeast *S. cerevisiae* cells ($C_Y = C_{cell} + C_{ICW}$)

The adhesion forces affect a relatively thick water layer (~3 nm) (Fig. 11, *b*). This is due to the cell surface structure including polar integral proteins and saccharides in the glycocalix layer of 20–50 nm in thickness. However, the $\langle T \rangle$ values (Table 2) are relatively large that suggest the absence of very strong confined space effects characteristic for nanopores in activated carbons with $S_{BET} > 1000$ m^2/g. Thus, the main

effects of the cell structures are due to polar and charged functionalities in "shaggy" macromolecular cell surface, which provide confined space effects in pores at $R > 0.5$ nm (Fig. 12).

Incremental PSD (Fig. 12, *b*) shows that mesopores at $2 < R < 25$ nm and macropores at $R = 25–40$ nm provide the main contribution to the pore volume. However, narrow pores more strongly contribute the specific surface area of cellular structures (Table 2, S_{uw} and S_{nano}). These structural characteristics are related to both intra- and extracellular waters. Notice that the ion percolation effects (i.e. throughout conductivity) are practically absent for the initial dry cells [50, 51].

CONCLUSIONS

Water in partially hydrated yeast cells is in a weakly associated state characterised by the chemical shift of the proton resonance at $\delta_H \approx 1–2$ ppm. A significant fraction of this water is weakly bound ($\Delta G > -0.8$ kJ/mol) to intracellular functionalities since it is frozen over a temperature range of 270–250 K. The behaviour of structured water in yeast cells strongly affected by organic solvents is similar to that in pores with mosaic hydrophobic/hydrophilic walls of activated carbons or mesoporous silicas. The structural (reflecting in changes in δ_H) and energetic (reflecting in changes in ΔG and freezing temperature) differentiations of intracellular water occur due to the influence of organic solvents. In the presence of nonpolar solvents (CCl_4 and benzene), a substantial part of weakly associated water ($\delta_H \approx 1–2$ ppm) transforms into strongly associated one ($\delta_H \approx 4–5$ ppm) and a portion of water becomes strongly bound ($\Delta G < -0.8$ kJ/mol, frozen at $T < 250$ K). This occurs to reduce the Gibbs free energy of the system on diminution of the contact area between water and nonpolar solvent fractions.

Polar organic solvents (acetonitrile, acetone, DMSO) capable to be dissolved in bulk water at any concentrations are characterised by a lower solubility in the interfacial or intracellular water. The structural and energetic differentiations of intracellular water occur in yeast cells with the presence of these polar solvents. A significant portion of intracellular water transforms into strongly associated state in which water molecules are in minimal contact with organic solvent molecules. Consequently, conditions of the formation of mixtures of organic solvents with intracellular water strongly differ from that in the bulk, and the aqueous and organic solvent phases can exist separately in the intracellular space over a wide range of their concentrations. The formation of mixtures occurs only at great excess of organic solvents; however, in this case the mixture exists separately from weakly associated water structures remaining in the cells.

The developed procedure allows us to estimate changes in the structural characteristics of intracellular pockets and features in changes in confined space of these pockets on cryopreservation of cells using different cryoprotectants. The obtained results on structural and energetic differentiations of intracellular water differently affected by nonpolar and polar solvents which differently displace bound water from various intracellular pockets and affect the clusterisation of intracellular water, can be useful for deeper insight into the processes occurring on cryopreservation of cells, tissues and other bioobjects, and for choice of novel cryoprotectants.

ACKNOWLEDGEMENTS

The authors are grateful to European Community, Seventh Framework Programme (FP7/2007-2013), Marie Curie International Research Staff Exchange Scheme (grant No 230790) for financial support.

REFERENCES

1. *Crowe J.H., Hoekstra F.A., Crowe L.M.* Anhydrobiosis // Annu. Rev. Physiol. – 1992. – V. 54. – P. 579–599.
2. *Dilks T.J.K., Proctor M.C.F.* The pattern of recovery of bryophytes after desiccation // J. Bryol. – 1974. – V. 8. – P. 97–115.
3. *Leopold A.C.* (Ed.) Membrane, metabolism and dry organisms // Comstock Pub. Assoc., 1986. – P. 188–209.
4. *Tunnacliffe A., de Castro A.G., Manzanera M.* Anhydrobiotic engineering of bacterial and mammalian cells: is intracellular trehalose sufficient // Cryobiology. – 2001. – V. 43, N 2. – P. 124–132.
5. *Becker M.E., Rapoport A.I., Kalakutsi L.B.* Detention of the cell vitality – Riga: Zinatne, 1987. – 239 p. (in Russian).
6. *Cameron R.E., Morelli F.A.* Viable microorganisms from ancient ross island and

tayler valley drill core // Antarctic J. U.S. – 1974. – V. 9. – P. 113–116.
7. *Gilichinsky D.* (Ed.) Viable microorganisms in permafrost // Russian Acad. Sci.: Pushchino, 1994. – 115 p.
8. *Gilichinsky D.A., Vorobyova E.A., Erokhina L.G. et al.* Long term preservation of microbial ecosystems in permafrost // Adv. Space Res. – 1992. – V. 12, N 5. – P. 225–263.
9. *Jones P.G., VanBogelen R.A., Neidhardt F.C.* Induction of proteins in response to low temperatures in *Escherichia coli* // J. Bacteriol. – 1987. – V. 169, N 5. – P. 2092–2095.
10. *Jones P.G., Inouye M.* The cold-shock response – a hot topic // Mol. Microbiol. – 1994. – V. 11, N 5. – P. 811–818.
11. *Gounot A.-M.* Bacterial life at low temperature, physiological aspects and biotechnological implications // J. Appl. Bacteriol. – 1991. – V. 71, N 5. – P. 386–397.
12. *Steponkus P.L., Uemura M., Webb M.S.* Membrane destabilization during freeze-induced dehydration // Curr. Topics Plant Physiol. – 1993. – V. 10. – P. 37–47.
13. *Steponkus P.L., Uemura M., Joseph R.A. et al.* Mode of action of the COR15a gene on the freezing tolerance of *Arabidopsis thaliana* // Proc. Natl. Acad. Sci. USA. – 1998. – V. 95. – P. 14570–14575.
14. *Strauss G., Hauser H.* Stabilization of lipid bilayer vesicles by sucrose during freezing // Proc. Natl. Acad. Sci. USA. – 1986. – V. 83, N 8. – P. 2422–2426.
15. *Anchordoguy T.J., Rudolph A.S., Carpenter J.F., Crowe J.H.* Modes of interaction of cryoprotectants with membrane phospholipids during freezing // Cryobiology. – 1987. – V. 24, N 4. – P. 324–331.
16. *Nanjo T., Kobayashi M., Yoshiba Y. et al.* Antisense suppression of proline degradation improves tolerance to freezing and salinity in *Arabidopsis thaliana* // FEBS Lett. – 1999. – V. 461, N 3. – P. 205–210.
17. *Antikainen M., Griffith M.* Antifreeze protein accumulation in freezing-tolerance cereals // Physiol. Plant. – 1997. –V. 99, N 3. – P 423–432.
18. *Armitage W.J., Juss B.K.* The influence of cooling rate on survival of frozen cells differs in monolayers and in suspensions // Cryo-Lett. – 1996. – V. 17, N 4. – P. 213–218.
19. *Karlsson J.O.M.* A theoretical model of intracellular devitrification // Cryobiology. – 2001. – V. 42, N 3. – P. 154–169.
20. *Hubalek Z.* Protectants used in the cryopreservation of microorganisms // Cryobiology. – 2003. – V. 46, N 3. – P. 205–229.
21. *Ashwood-Smith M.J., Farrant J.* (Eds.) Low Temperature preservation in medicine and biology – Pitman, Kent, England, 1980. – 323 p.
22. *Wang J.-H.* A comprehensive evaluation of the effects and mechanisms of antifreeze proteins during low-temperature preservation // Cryobiology. – 2000. – V.41, N 1. – P. 1–9.
23. *Tao D., Li P.H.* Classification of plant cell cryoprotectants // J. Theor. Biol. – 1986. – V. 123, N 3. – P. 305–310.
24. *Uzunova-Doneva T., Donev T.* Anabiosis and conservation of microorganisms // J. Culture Collect. – 2005. – V. 4, N 1. – P. 17–28.
25. *Turov V.V., Gun'ko V.M., Bogatyrev V.M. et al.* Structured water in partially dehydrated yeast cells and at partially hydrophobized fumed silica surface // J. Colloid Interface Sci. – 2005. – V. 283, N 2. – P. 329–343.
26. *Gun'ko V.M., Turov V.V., Bogatyrev V.M. et al.* Unusual properties of water at hydrophilic/hydrophobic interfaces // Adv. Colloid Interface Sci. – 2005. – V. 118, N 1–3. – P. 125–172.
27. *Surface Chemistry in Biomedical and Environmental Science, NATO Science Series II: Mathematics, Physics and Chemistry* / Eds. J.P. Blitz and V.M. Gun'ko. Dordrecht: Springer, 2006. – 444 p.
28. *Turov V.V., Gun'ko V.M., Tsapko M.D. et al.* Influence of organic solvents on interfacial water at surfaces of silica gel and partially silylated fumed silica // Appl. Surf. Sci. – 2004. – V. 229, N 1–4. – P. 197–213.
29. *Pople J.A., Schneider W.G., Bernstein H.J.* High-resolution nuclear magnetic resonance – New York: McGraw-Hill Book Company, 1959. – 501 p.
30. *Hindman J.C.* Proton rasonanse shift of water in the gas and liquid states // J. Chem. Phys. – 1966. –V. 44, N 12. – P. 4582–4592.
31. *Doremieux-Morin C., Heeribout L., Dumousseaux C. et al.* Study of constitutive superficial water of precipitated amorphous silicas using ^{1}H NMR: broad-line at 4 K and MAS at 300 K // J. Am. Chem. Soc. – 1996. – V. 118, N 51. – P. 13040–13045.

32. *Gun'ko V.M., Turov V.V., Shpilko A.P. et al.* Relationships between characteristics of interfacial water and human bone tissues // Colloids Surf. B. – 2006. – V. 53, N 1. – P. 29–36.
33. *Turov V.V., Gun'ko V.M., Zarko V.I. et al.* Weakly and strongly associated nonfreezable water bound in bones // Colloids Surf. B. – 2006. – V. 48, N 2. – P. 167–175.
34. *Bergna H.E.* (Ed.) Colloidal silica: fundamentals and applications – Taylor & Francis LLC, Salisbury, 2005. – P. 499–530.
35. *Gun'ko V.M., Turov V.V.* Structure of hydrogen bonds and ^{1}H NMR spectra of water at the interface of oxides // Langmuir. – 1999. – V. 15, N 19. – P. 6405–6415.
36. *Handbook of thermodynamic properties of individual substances* / Ed. V.P. Glushko – Moscow: Nauka, 1978. – 495 p. (in Russian).
37. *Strange J.H., Rahman M., Smith E.G.* Characterisation of porous solids by NMR // Phys. Rev. Lett. – 1993. – V. 71, N 21. – P. 3589–3591.
38. *Strange J.H., Mitchell J., Webber J.B.W.* Pore surface exploration by NMR // Magn. Reson. Imag. – 2003. – V. 21, N 3–4. – P. 221–226.
39. *Gallegos D.P., Munn K., Smith D.M., Stermer D.L.* A NMR technique for the analysis of pore structure: application to materials with well-defined pore structure // J. Colloid Interface Sci. – 1986. – V. 119, N 1. – P. 127–140.
40. *Aksnes D.W., Kimtys L.* ^{1}H and ^{2}H NMR studies of benzene confined in porous solids: melting point depression and pore size distribution // Solid State Nuclear Mag. Res. – 2004. – V. 25, N 1–3. – P. 146–152.
41. *Gun'ko V.M., Turov V.V., Leboda R. et al.* Adsorption, NMR and thermally stimulated depolarization current methods for comparative analysis of heterogeneous solid and soft materials // Langmuir. – 2007. – V. 23, N 6. – P. 3184–3192.
42. *Gun'ko V.M., Turov V.V., Zarko V.I. et al.* Comparative characterization of polymethylsiloxane hydrogel and silylated fumed silica and silica gel // J. Colloid Interface Sci. – 2007. – V. 308, N 1. – P. 142–156.
43. *Gun'ko V.M., Turov V.V., Leboda R. et al.* Comparative analysis of heterogeneous solid and soft materials by adsorption, NMR and thermally stimulated depolarisation current methods // Appl. Surf. Sci. – 2007. –V. 253, N 13. – P. 5640–5644.
44. *Provencher S.W.* A constrained regularization method for inverting data represented by linear algebraic or integral equations // Comp. Phys. Comm. – 1982 – V. 27, N 3. – P. 213–227.
45. *Gun'ko V.M., Turov V.V., Leboda R. et al.* Influence of organics on structure of water adsorbed on activated carbons // Adsorption. – 2005 – V. 11, N 1. – P. 163–168.
46. *Turov V.V., Gun'ko V.M., Leboda R. et al.* Influence of organics on structure of water adsorbed on activated carbons // J. Colloid Interface Sci. – 2002. – V. 253, N 1. – P. 23–34.
47. *Gun'ko V.M., Turov V.V., Turov A.V. et al.* Structural characteristics of ordered mesoporous silicas and properties of adsorbed pure water and water mixed with benzene or chloroform // Central Europ. J. Chem. – 2007. – V. 5. – P. 420–454.
48. *Physicochemistry of Nanomaterials and Supramolecular Structures* / Eds. A.P. Shpak and P.P. Gorbik – Kiev: Naukova Dumka, 2007. – 420 p. (in Russian).
49. *Chaplin M.* Water structure and science, http://www.lsbu.ac.uk/water/. – 2012.
50. *Gun'ko V.M., Turov V.V., Gorbik P.P.* Water at the Interfaces. – Kiev: Naukova Dumka, 2009. – 694 p. (in Russian).
51. *Turov V.V., Gun'ko V.M.* Clustered Water and Ways of its Applications. – Kiev: Naukova Dumka, 2011. – 313 p. (in Russian).

Received 08.10.2012, accepted 05.11.2012

Вплив органічних розчинників на поведінку внутрішньоклітинної води в клітинах дріжджів

В.М. Гунько, Т.В. Крупська, В.М. Барвінченко, В.В. Туров

Інститут хімії поверхні ім. О.О. Чуйка Національної академії наук України
вул. Генерала Наумова, 17, Київ, 03164, Україна, vlad_gunko@ukr.net

Методом ^{1}H ЯМР-спектроскопії з пошаровим виморожуванням об'ємної та зв'язаної води вивчено її стан в сухих (що містили близько 7 мас. % води) та частково регідратованих (при додаванні 10 мас. % води) дріжджових клітинах Saccharomyces cerevisiae при додаванні (10 мас.% або 2–3 г на грам сухих клітин) неполярних (C_6H_6, CCl_4) або полярних (CD_3CN, $(CH_3)_2CO$, $(CD_3)_2CO$, $(CH_3)_2SO$, $(CD_3)_2SO$) органічних розчинників. Показано, що неполярні розчинники витісняють частину води з вузьких пор в пори більшого розміру, а полярні – воду з широких мезопор в міжклітинний простір. Такі структурні відміни внутрішньоклітинної води супроводжуються її енергетичною диференціацією. Можна виділити чотири типи внутрішньоклітинної води: слабо- (хімічний зсув δ_H = 1–2 м.ч.) та сильноасоційовану (δ_H = 3–5 м.ч.), які можуть бути сильно- ($\Delta G < -0.8$ кДж/моль) або слабозв'язаними ($\Delta G > -0.8$ кДж/моль) з функціональними елементами клітини.

Влияние органических растворителей на поведение внутриклеточной воды в клетках дрожжей

В.М. Гунько, Т.В. Крупская, В.Н. Барвинченко, В.В. Туров

Институт химии поверхности им. А.А. Чуйко Национальной академии наук Украины
ул. Генерала Наумова, 17, Киев, 03164, Украина,vlad_gunko@ukr.net

Методом ^{1}H ЯМР-спектроскопии с послойным вымораживанием объемной и связанной воды изучено ее состояние в сухих (содержащих около 7 мас. % воды) и частично регидратированных (с добавлением 10 мас. % воды) дрожжевых клетках Saccharomyces cerevisiae при добавлении (10 мас. % или 2–3 г на грамм сухих клеток) неполярных (C_6H_6, CCl_4) или полярных (CD_3CN, $(CH_3)_2CO$, $(CD_3)_2CO$, $(CH_3)_2SO$, $(CD_3)_2SO$) органических растворителей. Показано, что неполярные растворители вытесняют часть воды из узких пор в поры большего размера, а полярные – воду из широких мезопор в межклеточное пространство. Такие структурные различия внутриклеточной воды сопровождаются ее энергетической дифференциацией. Можно выделить четыре типа внутриклеточной воды: слабо- (химический сдвиг δ_H = 1–2 м.д.) и сильноассоциированную (δ_H = 3–5 м.д.), которые могут быть сильно- ($\Delta G < -0.8$ кДж/моль) или слабосвязанными ($\Delta G > -0.8$ кДж/моль) с функциональными элементами клетки.